Original Article

Dust Resuspension from Fabrics Exposed to Airflow

Jie Feng [a], Tsz Wai Lai [b], Sau Chung Fu [b, *], Ka Chung Chan [b], Chun-Ho Liu [a], Christopher Y.H. Chao [b, c]

[a] Department of Mechanical Engineering, The University of Hong Kong, Hong Kong, China

[b] Department of Building Environment and Energy Engineering, The Hong Kong Polytechnic University, Hong Kong, China

[c] Department of Mechanical Engineering, The Hong Kong Polytechnic University, Hong Kong, China

[*] Corresponding author. E-mail address: schung.fu@polyu.edu.hk (S.C. Fu).

ABSTRACT

Dust resuspension from four typical fabrics (cotton, linen, silk, and polyester) exposed to airflow with common velocities within 0 ~ 10 m/s, including a moving fabric case and a fixed fabric case, was experimentally studied in this paper. A set of empirical correlations, involving air velocity, fabric motion mode, fabric type, and airflow duration was developed to describe and predict the moving fabric case. It was found that a stronger-than-expected resuspension was triggered by short-term accelerating airflow. The resuspension enhancement of over 90% was reported for the moving fabrics compared with the fixed ones. Fabric motion induced by airflow was proposed to account for these resuspension findings. Fabric acceleration was then demonstrated to be a key factor in evaluating the resuspension for such a scenario. This paper not only reveals an inconspicuous phenomenon of dust resuspension from fabrics under the impact of airflow and consequent fabric motion, but also provides a theoretical basis for particulate matter assessment and regulation.

KEYWORDS: particulate matter, dust, resuspension, fabric, airflow, flutter.

1. Introduction

Dust resuspension, a non-exhaust emission of particulate matter (PM), is poorly regulated and often underestimated. In fact, it is one of the largest contributors to PM exceedances in many regions (Rienda and Alves 2021). More notably, its contribution is undesirably increasing, as opposed to well-regulated exhaust emissions (Fussell et al. 2022; Farahani et al. 2022). This issue should be taken seriously because a compelling body of evidence has indicated that exposure to PM especially inhalable PM (10 microns or less in diameter, PM_{10}) is strongly associated with adverse health effects such as respiratory, cardiovascular, neurodegenerative, digestive, and genitourinary diseases (Zhang et al. 2023; Song et al. 2022; Calderon-Garciduenas and Ayala 2022; Sun et al. 2019; Zhou et al. 2018; Shiraiwa et al. 2017). Furthermore, when contaminated dust is resuspended and inhaled by people, it will greatly increase the risk of pathogen transmission (Qi et al. 2022; Lai et al. 2017; Knibbs et al. 2012). Over the past year, an outbreak of melioidosis (a fatal infection caused by the bacterium Burkholderia pseudomallei) in Hong Kong has drawn public attention. Reported cases tend to be associated with occupational activities involving exposure to contaminated soil, like construction work. Inhalation of contaminated dust is now recognized as one of the melioidosis transmission routes (Leung et al. 2023), promoting the urgent need for more studies on dust resuspension.

Dust can be resuspended and carried by wind (Henry and Minier 2014), which is almost everywhere in our daily life. This wind-induced resuspension has been extensively studied over the past few decades, including experimental work (Rondeau et al. 2021; Kim et al. 2016; Barth et al. 2014; Jiang et al. 2008; Ibrahim et al. 2003; Wu et al. 1992) and model development (Nasr et al. 2020; You and Wan 2014; Goldasteh et al. 2013; Guingo and Minier 2008; Reeks and Hall 2001; Ziskind et al. 1997). For the simplest case, a single particle being resuspended by wind from a flat surface, the basic mechanism has been clarified from various perspectives. For instance, from the perspective of a force/moment balance, this process is explained as a situation where the aerodynamic force/moment overcomes the adhesive force/moment. However, the wind-induced resuspension in real scenarios is more complicated. It can be

influenced by many factors related to airflow, particles, and surfaces. Thus, many studies have been devoted to enriching the resuspension theory by including these factors. Some recent studies (Theron et al. 2022, 2020) noted that most previous studies considered the steady-state airflow only, ignoring the transient accelerating airflow. The latter is inevitable in many real-life situations, such as during a wind gust and a fan startup. To depict the temporal evolution of resuspension during this airflow acceleration period, Theron et al. (2022, 2020) developed an experimental methodology involving both air velocity signal acquisition and resuspension kinetics measurement, and then demonstrated that high airflow accelerations account for high resuspension rates. These results provided new insights into the interpretation of wind-induced resuspension, but only for particles being resuspended from rigid surfaces.

When the surface is flexible, the wind-induced resuspension phenomenon becomes more complex, as the surface would move, vibrate, and deform when exposed to airflow. For example, leaf species with more flexible structures have been reported to result in higher resuspension rates possibly due to their wind-induced erratic motion (Zhang et al. 2020). Consequently, although vegetation is effective in reducing PM pollution concentrations, the sediment on leaves could also be resuspended into the air as a secondary source of contaminants, depending on leaf characteristics and weather conditions such as wind speed (Pace et al. 2021). Obviously, existing wind-induced resuspension models based on rigid surfaces are not able to fully estimate the real situation with such accompanying surface motion. In addition, the aforementioned accelerating airflow will add complexity, but it is even less understood.

These flexible surfaces appear everywhere in our daily life. Fabric is an example that would be the most closely in contact with human beings, such as clothes, mattresses, carpets, towels, curtains, or tents, etc., in both indoor and outdoor environments. Due to their closeness to us, several investigations involving both contaminated fabrics and airborne PM have been carried out for human exposure assessment (Kvasnicka et al. 2022; Licina and Nazaroff 2018; Boor et al. 2015). A full-scale chamber study was conducted by Boor et al. (2015) to show that dust resuspension from mattresses increased with the intensity of volunteers' movements as characterized by surface vibrations. More vigorous fabric motion was found to enhance the clothing release fraction in another chamber study performed by Licina

and Nazaroff (2018). It was confirmed that clothing can act as a path for airborne PM. Moreover, this function of clothing boosted the development of a computational modeling framework for contaminants assessment during the COVID-19 pandemic (Kvasnicka et al. 2022).

From the above, it can be expected that wind may lead to fabric motion, thereby enhancing dust resuspension and inhalation exposure. For indoors, although typical air velocities are not high due to human comfort needs, occasional high air velocities cannot be ignored here, e.g., the wind near air vents, the wind coming in from windows/doors, and the wind generated by household appliances such as hair dryers or vacuum cleaners. For outdoors, this wind-related phenomenon occurs more frequently and may have a greater impact on air quality, especially when fabrics with high dust loads are involved, such as on roads, factories, and construction sites. However, most of such fabric studies to date have focused on human activities, and to the best of our knowledge, there are no previous parametric studies on dust resuspension from fabrics under the impact of airflow and consequent fabric motion. The absence of a description of this phenomenon may limit the practical value of existing resuspension models.

To fill this knowledge gap, an experimental study on dust resuspension from fabrics exposed to airflow is presented in this paper. Dust resuspension and fabric motion were both recorded. The period during which the airflow accelerated to the target velocity was considered and distinguished from the steady state. A set of empirical correlations, involving air velocity, fabric motion mode, fabric type, and airflow duration was developed to predict dust resuspension for this scenario. A wholly fixed fabric case was used for comparison under the same experimental conditions. The flow-induced motion characteristics of fabrics were quantified to elucidate their contribution to dust resuspension.

2. Materials and methods

Resuspension experiments were conducted in a subsonic wind tunnel (C15, Armfield, UK) at an ambient temperature of 23.3 ± 0.5 ℃ and a relative humidity of 68 ± 1 %. The dimensions of the working section were 150 mm × 150 mm × 455 mm (Width × Height × Length). The leading edge of the rectangular fabrics (with dust loaded on the top surface) was fixed on the holder and the trailing edge was

free, while the fabrics were wholly fixed on a flat surface in the control experiment (Figure 1a). Four common and representative fabrics were adopted in the present work: cotton, linen, silk, and polyester (Figure 1b). Surface morphologies of the fabrics were observed using a scanning electron microscope (Gemini 500, Zeiss, Germany). Flexural rigidity per unit width of the fabrics was assessed according to the Chinese Standard GB/T 18318.1-2009. For our research motivation, Arizona Test Dust (ISO 12103-1, A1 Ultrafine, Powder Technology Inc., USA) was used in this work as more than 20% and 95% of the dust were less than 2.5 microns and 10 microns in size respectively.

Figure 1

The dust was deposited on the fabrics before the resuspension experiments. It was dispersed via an electric spraying system (PF101, DASHING, China) with a constant flow rate and then the gravitational deposition was carried out in a chamber with a volume of 125 L (Figure 1c). The fabrics with the same effective test area of 60 mm × 30 mm were placed on the floor of the chamber. An initial dust load of 15 g/m^2 was moderately selected for our study based on indoor and outdoor field investigation findings by other researchers (Wu et al. 2021; Jeong et al. 2020; Gustafsson et al. 2019; Roberts et al. 2004), representing a high level for indoor environments and a low level for outdoor environments (Table S1). The duration of each deposition was controlled to 1 hour including the first 5 minutes of spraying. This consistent deposition method enabled the dust load of approximately 15 g/m^2 on each fabric (Table S1), demonstrating the uniformity and repeatability of dust deposition in this study. The initial deposition height (δ) in this study can be estimated as follows (Lee et al. 2019),

$$\delta = \frac{6m_0}{\pi\rho(1-\varepsilon)} \quad (1)$$

where m_0 is the initial dust load (= 15 g/m^2 in this study), ρ is the dust density (= 2.65 g/cm^3 provided by the manufacturer specification sheet), ε is the porosity of the dust structure (= 0.75 for sticky particles under gravitational settling conditions), and thus the multilayer deposition was identified in this study based on the criteria of $\delta \geq 2d$ (Lee et al. 2019) where d is the dust diameter (the median diameter is 4.34 μm provided by the manufacturer specification sheet).

More detailed experimental setup can be found in Figure S1. The chosen air velocity range was 0 ~ 10 m/s according to the Beaufort scale of 0 ~ 5, excluding extreme weather conditions above strong breeze, which represented the natural wind magnitudes commonly encountered in real-life scenarios. The target air velocity (U) studied in this paper was set to 2, 4, 6, 8, and 10 m/s by an inverter speed control unit, and the real-time air velocity was monitored by an anemometer (Model 9565, TSI, USA) placed at the entrance of the working section (Figure S1a). The evolution of air velocity over time is plotted in Figure 1d and the trends are similar regardless of fabric type or fabric motion. Air velocity inevitably goes through an acceleration period before reaching a steady state at U. We highlighted this acceleration period in this work and defined its duration (t_0) as the first time when the real-time air velocity reaches or exceeds 99% of U (the value of 99% was set to consider a reasonable slight fluctuation in U when operating in the wind tunnel). In this study, t_0 was 5 seconds in order to keep our airflow mean acceleration range (i.e., 0.4 ~ 2.0 m/s^2) within the typical range in the previous related study (Theron et al. 2022), and then using t_0 as a reference, the airflow duration (t), i.e., from blower on to blower off, was set to 5 s, 10 s, 15 s, and 20 s, i.e., $t = t_0 + nt_0$, (n = 0, 1, 2, 3), which allowed both the acceleration period (n = 0) and the steady state ($n > 0$) to be considered.

An analytical balance (ABP 200-5DM, Kern, Germany) was employed to weigh the fabrics and dust (Figure S1a) so that the remaining fraction, defined as the ratio of the weight of remaining dust on the fabrics at U to that at U = 0 m/s, was used to evaluate the overall resuspension. The remaining fraction was always 1 at the beginning when U = 0 m/s. The resuspension fraction can thus be counted as 1 minus the remaining fraction without extra air concentration measurements in this study. In addition, to prevent the weighed fabrics from repeatedly experiencing the airflow acceleration period at the same U, their remaining fractions at different t (i.e., 5 s, 10 s, 15 s and 20 s) were obtained separately from four pieces of fabric treated with the consistent deposition method, rather than from the same piece again.

Airflow caused the fabrics' free parts to move, so a high-speed camera (VEO-L, Phantom, USA) was installed beside the wind tunnel to record the fabric motion from a side view (Figure S1b). The movements of six markers spaced 10 mm apart on the long side of the fabrics (Figure S1c) were captured

by the high-speed camera at 500 frames per second (500 fps) for the fabric motion analysis. The calculations of fabric acceleration (a_F) and the maximum ($a_{F,\,max}$) discussed in this paper were the same as our previous work (Feng et al. 2023).

3. Results and discussion

3.1. Dust resuspension from flow-induced moving fabrics

Fabrics move when exposed to airflow, and the occurrence of flutter is a distinctive feature of their motion, such as a fluttering flag (Argentina and Mahadevan 2005). In this study, the critical air velocities (U_C) at which the four moving fabrics (cotton, linen, silk, and polyester) began to flutter were measured to be 4.51 m/s, 3.21 m/s, 1.85 m/s, and 7.67 m/s respectively. Due to the significant difference in fabric motion modes before and after fluttering, the generalization of dust resuspension in this section is divided into two stages: $U < U_C$ and $U \geq U_C$. Based on our previous work (Leung et al. 2017; Fu et al. 2013), it is now assumed in this paper that the resuspension problem in both stages can also be described by a cumulative distribution function (CDF) in the form of an error function (erf). More details on this mathematical description can be found in Figure S2. The dependent variable is the remaining fraction, expressed as 1 - CDF, while the independent variable is the dimensionless U-related term of $\ln(U/U_C)^3$. The cubic form of air velocity was chosen as it was optimal in our fitting attempts. By fitting the experimental results at the steady state (n = 1, 2, 3) shown in Figure 2, a set of empirical correlations for describing dust resuspension from flow-induced moving fabrics was developed as follows:

$$1 - CDF\left[ln\left(\frac{U}{U_C}\right)^3\right] = \frac{1}{2}\left\{1 - erf\left[\frac{ln\left(\frac{U}{U_C}\right)^3 - A}{B\sqrt{2}}\right]\right\} \quad (2a)$$

where

$$A = \begin{cases} -0.79 lnU_C^3 + 12 \cdot \dfrac{1}{t_0 + nt_0} + 3.92, \ U < U_C, \\ -0.52 lnU_C^3 + 12 \cdot \dfrac{1}{t_0 + nt_0} + 0.44, \ U \geq U_C, \end{cases} \qquad (n = 1, 2, 3, \ldots)$$

$$B = -0.19 lnU_C^3 + 2.84, \qquad U < U_C \ \ or \ \ U \geq U_C$$

where A and B are the mean and standard deviation of the log-normal distribution, respectively. U_C and t were found to be two important factors influencing the distribution. The sudden drops in the remaining fraction in Figure 2 when U exceeds U_C confirm the necessity of the separate discussion by using $U = U_C$ as the dividing line. U_C also provides a way to link the fabric type to the above mathematical description since different fabrics showed different U_C under the same experimental conditions. On the other hand, the time dependence of the resuspension rate in the typical flow-induced case (i.e., from a rigid flat plate) has been suggested to be approximately $1/t$ decay (Reeks and Hall 2001; Reeks et al. 1988). During the fitting attempts, we observed that the parameter A was sensitive to the fabric motion mode (reflected by $U < U_C$ or $U \geq U_C$), the fabric type (reflected by U_C), and t, while the parameter B tended to respond only to the fabric type (reflected by U_C). For analogy with the U-related term $(\ln(U/U_C)^3)$ and the typical time dependence ($1/t$ decay), the U_C-related term of $\ln U_C^3$ and the t-related term of $1/(t_0 + nt_0)$ were selected for the fitting. The results indicate that the parameter A is linear with both $\ln U_C^3$ and $1/(t_0 + nt_0)$, while the parameter B is linear with $\ln U_C^3$, as expressed in Eq. (2a). The consequent distribution (Eq. (2a)) is plotted in Figure 2, showing good agreement with the experimental results at the steady state (n = 1, 2, 3). It can be seen from Figure 2 that the distribution curve for each fabric determined by the given U_C and t is shifted to the left by a certain amount due to the occurrence of flutter ($U \geq U_C$). The leftward shift of the curve means that the resuspension occurred earlier than expected on the scale of U, demonstrating the potential for flutter to enhance resuspension.

Figure 2

When n = 0, the air velocity during this acceleration period was not constant, making its mathematical description more difficult. The above-mentioned Eq. (2a), which was derived from the steady-state

experimental results (also experienced the airflow acceleration period), provides an approach to predicting the results for $n = 0$ in reverse. If they all followed the same pattern, the prediction for $n = 0$ using Eq. (2a) with U should be in good agreement with its experimental data. However, the poor fitting in Figure 2 shows that it does not work and is apparently underestimated. This special case of $n = 0$ seems not to follow the resuspension pattern exhibited by Eq. (2a). Therefore, Eq. (2a) needs to be further refined to include the airflow acceleration period of $t = t_0$. During the equation modification, we found that all prediction deviations could be represented by an equivalent reduction in the parameter A as expressed in Eq. (2b):

$$1 - CDF\left[ln\left(\frac{U}{U_C}\right)^3\right] = \frac{1}{2}\left\{1 - erf\left[\frac{ln\left(\frac{U}{U_C}\right)^3 - A'}{B\sqrt{2}}\right]\right\} \quad (2b)$$

where

$$A' = A - 0.98, \qquad (n = 0)$$

where A' is the modified A in Eq. (2a) for $n = 0$. Eq. (2b) is plotted in Figure 3 and agrees better with the experimental results at $t = t_0$. The "non-accidental" leftward shift of these curves confirms that there is an unknown resuspension mechanism within the airflow acceleration period. It can be deduced that the resuspension at the steady state may have occurred in advance during this period in which most air velocities have not even reached U. The influence of accelerating airflow mentioned in the introduction could be the reason. When the airflow was accelerating, the motion of the moving fabrics was also accelerating. The coupling of these two accelerating events cannot be ignored, as suggested by our experimental results and empirical correlations. The term of -0.98 in Eq. (2b) is an indicator of the resulting stronger-than-expected resuspension in this study, but the underlying mechanism needs to be clarified by our fabric motion analysis later.

Figure 3

3.2. Comparison between moving fabrics and fixed fabrics

Figure 4 demonstrates the resuspension enhancement of the moving fabrics compared to the fixed fabrics under the same experimental conditions, as reflected by the difference in remaining fractions, ΔRF (= $RF_{fixed\ case}$ - $RF_{moving\ case}$). Detailed resuspension results for both cases are reported in Figure S3. Within the range of $U < U_C$, the ΔRF is generally at a low level but increases with the air velocity. Slight vibrations of the moving fabrics could be one of the main causes for this rising trend, though the fabrics did not flutter at that time. When the fabrics flutter, the ΔRF increases dramatically, up to more than 0.9, illustrating the prominent contribution of the fluttering fabrics to enhancing resuspension. Moreover, Figure S3 suggests that differences caused by fabric motion were dominant in this study, rather than those caused by fabric surface morphology.

From the perspective of t, the enhancement when $t = t_0$ is not far behind the steady state, and even prevails at high air velocities, especially at U = 10 m/s (Figure 4). This finding reveals the potential of a high-speed wind gust to accelerate pollutants in a short time. In the fixed fabric case, dust was hardly resuspended when $t = t_0$, even at U = 10 m/s, while the resuspension was improved a bit as t increased. By contrast, we can infer that the superiority of the moving fabrics over the fixed fabrics during the same acceleration period would be due to the additional accompanying fabric motion, which also supports the mathematical description in the previous section.

Figure 4

3.3. Flow-induced fabric motion analysis

The motion analysis for the moving fabrics is presented in this section to elucidate the reported resuspension phenomenon. Since the motion process was similar for all the fabrics exposed to airflow in this study, the motion of cotton fabric is displayed and discussed here as an example (Figure 5a-c). The stacked images of traces (at U = 4 m/s and 6 m/s, representing the non-fluttering and fluttering cases respectively) recorded by the high-speed camera within different time periods are shown in Figure 5a. When t = 0 s, the fabric drooped naturally and remained still. As time went by, the air velocity increased

from 0 to U. The U_C of the cotton fabric appeared during the airflow acceleration period when U = 6 m/s, hence t_0 is divided into 2 stages (t = 0 ~ 2.5 s and 2.5 ~ 5 s) to be displayed to distinguish the non-fluttering and fluttering cases more clearly. When t = 0 ~ 2.5 s, the fabric was lifted by the airflow, as reflected by the traces of the six markers. The difference between U = 4 m/s and U = 6 m/s within this stage is that the fabric was lifted a little higher at U = 6 m/s. However, their traces start to differ a lot within the next stage of t = 2.5 ~ 5 s. The traces show that the fabric remained straight with slight vibrations after being lifted at U = 4 m/s, while it evolved to flutter with greater amplitudes after being lifted at U = 6 m/s. These two motion modes were respectively maintained within the subsequent steady state of t = 5 ~ 20 s. It can be seen from Figure 5a that the fabric motion mode at the steady state has already occurred in advance during the airflow acceleration period.

To quantify the fabric motion modes shown in Figure 5a, the fabric acceleration versus time is depicted in Figure 5b. According to Newton's second law of motion, this acceleration can reflect a dust removal force directly exerted by a moving fabric. Since Figure 5a illustrates that the marker (P6) farthest from the fixed end has the longest trace and the largest motion amplitude, P6 is used for the fabric acceleration analysis in this paper to indicate the overall motion. As demonstrated in Figure 5b, a_F at U = 4 m/s fluctuates over time within a low level below 45 m/s^2, while a_F at U = 6 m/s undergoes a surge in the first 5 s and then keeps fluctuating within a high level of up to nearly 1200 m/s^2. The surge can be explained by the fact that U_C was exceeded when the airflow was accelerating, and the fabric state was switched to fluttering. This evolution is enlarged in Figure 5c so we can clearly see that a_F at U = 6 m/s (the fluttering case) rises abruptly to the high level (about 0.1 s). Whereas there is no obvious change in a_F at U = 4 m/s (the non-fluttering case). Figure 5b also shows that $a_{F,\,max}$ within each 5 s is very close and sometimes $a_{F,\,max}$ in the first 5 s is even stronger than that in the second 5 s, which is consistent with the finding from the trace-stacked images (Figure 5a) that the fabric motion mode at the steady state occurs earlier. It follows that the fabric's ability to resuspend dust within each 5 s should be comparable, because its $a_{F,\,max}$ can reflect its maximum dust removal force. The results of $a_{F,\,max}$ for all fabrics are presented in Figure S4 and are close and about the same magnitude within each 5 s. They explained for the reported stronger-than-

expected resuspension during the airflow acceleration period, i.e., the accelerating airflow also accelerated the moving fabrics to their steady-state motion levels. Recalling the results from the comparison with the fixed fabric case in Figure 4, it is concluded that the accompanying fabric motion amplifies the resuspension-promoting effect of the accelerating airflow in the moving fabric case.

Figure 5

The flow-induced motion performance of fabrics is also related to their mechanical properties. For example, a fabric with less flexural rigidity is normally considered softer, and vice versa. Depending on the airflow direction, the longitudinal flexural rigidity (Σ) is discussed in this work and its magnitude order is found to correspond to U_C, i.e., silk < linen < cotton < polyester (Figure 5d). Moreover, there is a linear relationship between U_C^3 and Σ as listed below:

$$U_C^3 = 33.41\Sigma - 7.43, \qquad 0.43\ \text{mN} \cdot \text{cm} \leq \Sigma \leq 13.90\ \text{mN} \cdot \text{cm} \tag{3}$$

providing further evidence for the assumption that U_C represents the fabric type in Eq. (2a) and Eq. (2b). The cubic form of air velocity here also corresponds to the above mathematical description. Therefore, the U_C^3 - Σ relationship connects Eq. (2a), Eq. (2b) and Eq. (3). This set of empirical correlations is effective for quickly predicting the dust resuspension from the flow-induced moving fabrics and offers useful information for understanding the mechanisms behind the phenomenon.

3.4. Link between flow-induced fabric motion and dust resuspension

The results of $a_{F,\,max}$ for all fabrics during the experiments are plotted versus their corresponding remaining fractions in Figure 6. An exponentially decaying trendline is drawn as a guide to the eye. The overall trend is that the remaining fraction decreases as $a_{F,\,max}$ increases, and levels off when approaching 0. More specifically, the resuspension results are sensitive when $a_{F,\,max}$ is less than 2000 m/s^2, and thereafter close to their limits and vary little even if their $a_{F,\,max}$ continues to increase substantially.

Figure 6

When the fabrics have not started to flutter, $a_{F,\,max}$ is nearly 0, but their remaining fractions differ by up to almost 0.4. The diversity brought by different U (shown in different colors in Figure 6) within the

"non-fluttering region" is attributed to different aerodynamic forces on the dust. For instance, the polyester fabric did not flutter at $U = 6$ m/s due to its high U_C but had the strongest aerodynamic force within this region compared to other non-fluttering fabrics at the lower U. Besides, t was a factor but need not be discussed in this section, as t had little impact on $a_{F,\,max}$ (Figure 5b and Figure S4). After the "non-fluttering region", the silk, linen, cotton, and polyester fabrics begin to flutter at different U in sequence with their higher $a_{F,\,max}$, thereby leading to their declining remaining fractions, as depicted in Figure 6. Only high U cases such as $U = 8$ m/s and $U = 10$ m/s can enter the region where $a_{F,\,max}$ exceeds 2000 m/s^2, suggesting that for a specific fabric, the faster U accounts for the higher $a_{F,\,max}$. However, for different fabrics, their $a_{F,\,max}$ is different even at the same U, which depends on their mechanical properties. For example, Figure 6 shows that the "softer" silk fabric at $U = 6$ m/s and $U = 8$ m/s already has a comparable $a_{F,\,max}$ to that of the "more rigid" polyester fabric at $U = 8$ m/s and $U = 10$ m/s respectively. In general, the fabrics with lower U_C tend to achieve higher $a_{F,\,max}$ at the same U, and the difference becomes larger as U increases. Although their motion performance under the same wind conditions is different, the relationship between their resuspension and maximum acceleration results, regardless of U, is basically in line with the trend displayed in Figure 6. It confirms the previously stated explanation for the significant resuspension at $t = t_0$ in terms of the fabric motion. This section not only puts forward the effective range of force by fabrics required to resuspend dust, but also implies that the fabric acceleration plays a crucial role in such a flow-induced resuspension.

4. Conclusions

This work reports the resuspension results of dust from four typical fabrics (cotton, linen, silk, and polyester) exposed to airflow with common velocities within 0 ~ 10 m/s, giving a reference for air pollution assessment in practical scenarios. The development of empirical correlations for the flow-induced moving fabric case offers a feasible solution for describing and predicting this complex resuspension phenomenon under the different conditions of air velocity, fabric motion mode, fabric type, and airflow duration. In particular, this set of empirical correlations makes it possible to use the target air

velocity to effectively estimate the stronger-than-expected resuspension during the inevitable airflow acceleration period, proposing that the time-segmented approach based on this period in this work deserves to be applied in similar experimental studies in the future. This finding also demonstrates a significant contribution of short-term accelerating airflow to dust resuspension from fabrics, as the fabrics are moved by the airflow, suggesting the potential for wind gusts in real-world scenarios to trigger high levels of air pollutants even in a short time. Not only the superior overall resuspension enhancement of the moving fabrics, but also their resuspension-promoting effect by the accelerating airflow, are confirmed in this work compared to the fixed fabrics. These conclusions can be useful for the scenarios previously mentioned in the introduction, such as the melioidosis outbreak on construction sites and the occasional windy cases in rooms with many softer fabrics. Furthermore, the motion of fabrics exposed to airflow is summarized and quantified, which helps interpret the reported resuspension results and lay out guidelines for the removal force exerted by fabrics. This paper provides new insights into evaluating and controlling the PM exceedances in daily life as well as the design and optimization of decontamination applications.

Some limitations and future work are elaborated below.

First, although the term of -0.98 in Eq. (2b) is shown as an indicator of the stronger-than-expected resuspension during the airflow acceleration period, this number may not be for all scenarios because the airflow may accelerate differently. More solid conclusions can be further obtained through experiments with different airflow acceleration settings, such as different acceleration durations under the same air velocity. Furthermore, the airflow in real-life scenarios is usually more chaotic than the unidirectional airflow in our wind tunnel. The fabric motion induced by the variable-speed airflow (i.e., airflow temporal instability) has been found in this work to cause significant dust resuspension. It can be expected that the variable-direction airflow (i.e., airflow spatial instability) may also contribute to the resuspension, suggesting its practical value as a future investigation.

Second, only a representative dust load (similarly, only a multilayer deposition) was investigated in this work. According to Eq. (1) and its criteria mentioned previously, different dust loads will lead to different

deposition types. As the deposition type changes from sparse monolayer to dense monolayer to multilayer, the dust also undergoes a transition from individual events to collective events (Henry et al. 2023). Specifically, only particle-fluid and particle-surface interactions may be involved under lower dust loads, whereas particle-particle interactions, e.g., particle collisions, may emerge with rising dust loads. The resuspension behavior of monolayer dust with lower dust loads would be less complex, but no less important since it could also be included in the multilayer deposition. Even though this paper elicits some informative results for the multilayer deposition, lower dust loads (i.e., monolayer deposition) need to be investigated in the future to get a full picture of this scenario.

Third, fabric surface morphology (e.g., surface roughness and surface pattern) has not been focused on in the present work, because Figure S3 suggests that the differences in resuspension caused by fabric motion were dominant in this study, rather than those caused by the fabric surface morphology. However, since surface morphology has long been recognized as one of the important factors influencing resuspension, it still deserves further investigation. Although it did not show an obvious role on its own under our conditions, its synergistic effect with the fabric motion on resuspension is not yet clear. More microscopic studies should be conducted.

Last but not least, fabric acceleration was identified in this work as an important factor for resuspension (demonstrated by a clear measured trend), but it was not clear about the influence of simultaneous aerodynamic forces on the dust, which should also contribute theoretically. Although they were presented to have little contribution in the fixed fabric case, it is believed that they may have changed in the moving fabric case. However, the fabric motion and the simultaneous aerodynamic forces were not easily separated distinctly into the resuspension discussion under the experimental conditions of this work. In addition to the fact that our fabrics were similarly sensitive to dust resuspension, their high resuspension results here usually corresponded to high air velocity and high fabric acceleration at the same time, which makes it difficult to distinguish whose contribution was greater. The reported results from direct measurements have practical implications, but a thorough understanding of this phenomenon still requires a more complete theoretical study in the future.

Supplemental information

Table S1, Figure S1, S2, S3 and S4.

Disclosure statement

The authors declare no competing financial interest.

Funding

This work was supported by the General Research Fund (GRF) (project no. 17203220) and the Collaborative Research Fund (CRF) (projects no. C7064-18G & C1105-20G) granted by the Research Grants Council of the Hong Kong Special Administrative Region, China, and internal grants from The Hong Kong Polytechnic University (projects no. P0041489 & P0045922).

References

Argentina, M., and L. Mahadevan. 2005. "Fluid-flow-induced flutter of a flag." *Proceedings of the National Academy of Sciences of the United States of America* 102 (6):1829-1834. doi: 10.1073/pnas.0408383102.

Barth, T., J. Preuß, G. Müller, and U. Hampel. 2014. "Single particle resuspension experiments in turbulent channel flows." *Journal of Aerosol Science* 71:40-51. doi: 10.1016/j.jaerosci.2014.01.006.

Boor, B. E., M. P. Spilak, R. L. Corsi, and A. Novoselac. 2015. "Characterizing particle resuspension from mattresses: Chamber study." *Indoor Air* 25 (4):441-456. doi: 10.1111/ina.12148.

Calderon-Garciduenas, L., and A. Ayala. 2022. "Air pollution, ultrafine particles, and your brain: Are combustionnanoparticle emissions and engineered nanoparticles causingpreventable fatal neurodegenerative diseases and commonneuropsychiatric outcomes?" *Environmental Science & Technology* 56 (11):6847-6856. doi: 10.1021/acs.est.1c04706.

Farahani, V. J., A. Altuwayjiri, S. Taghvaee, and C. Sioutas. 2022. "Tailpipe and nontailpipe emission factors and source contributionsof pm(10) on major freeways in the los angeles basin." *Environmental Science & Technology* 56 (11):7029-7039. doi: 10.1021/acs.est.1c06954.

Feng, J., C. T. Wang, Y. Zhang, K. C. Chan, C. H. Liu, C. Y. H. Chao, and S. C. Fu. 2023. "Particle resuspension from a flow-induced fluttering flexible substrate." *Powder Technology* 415:12. doi: 10.1016/j.powtec.2022.118163.

Fu, S. C., C. Y. H. Chao, R. M. C. So, and W. T. Leung. 2013. "Particle resuspension in a wall-bounded turbulent flow." *Journal of Fluids Engineering-Transactions of the Asme* 135 (4):9. doi: 10.1115/1.4023660.

Fussell, J. C., M. Franklin, D. C. Green, M. Gustafsson, R. M. Harrison, W. Hicks, F. J. Kelly, F. Kishta, M. R. Miller, I. S. Mudway, F. Oroumiyeh, L. Selley, M. Wang, and Y. F. Zhu. 2022. "A review of road traffic-derived non-exhaust particles: Emissions, physicochemical characteristics, health risks, and mitigation measures." *Environmental Science & Technology* 56 (11):6813-6835. doi: 10.1021/acs.est.2c01072.

Goldasteh, I., G. Ahmadi, and A. R. Ferro. 2013. "Monte carlo simulation of micron size spherical particle removal and resuspension from substrate under fluid flows." *Journal of Aerosol Science* 66:62-71. doi: 10.1016/j.jaerosci.2013.07.012.

Guingo, M., and J. P. Minier. 2008. "A new model for the simulation of particle resuspension by turbulent flows based on a stochastic description of wall roughness and adhesion forces." *Journal of Aerosol Science* 39 (11):957-973. doi: 10.1016/j.jaerosci.2008.06.007.

Gustafsson, M., G. Blomqvist, I. Jarlskog, J. Lundberg, S. Janhall, M. Elmgren, C. Johansson, M. Norman, and S. Silvergren. 2019. "Road dust load dynamics and influencing factors for six winter seasons in stockholm, sweden." *Atmospheric Environment-X* 2:12. doi: 10.1016/j.aeaoa.2019.100014.

Henry, C., and J. P. Minier. 2014. "Progress in particle resuspension from rough surfaces by turbulent flows." *Progress in Energy and Combustion Science* 45:1-53. doi: 10.1016/j.pecs.2014.06.001.

Henry, C., J. P. Minier, and S. Brambilla. 2023. "Particle resuspension: Challenges and perspectives for future models." *Physics Reports-Review Section of Physics Letters* 1007:1-98. doi: 10.1016/j.physrep.2022.12.005.

Ibrahim, A. H., P. F. Dunn, and R. M. Brach. 2003. "Microparticle detachment from surfaces exposed to turbulent air flow: Controlled experiments and modeling." *Journal of Aerosol Science* 34 (6):765-782. doi: 10.1016/s0021-8502(03)00031-4.

Jeong, H., J. Y. Choi, J. Lim, and K. Ra. 2020. "Pollution caused by potentially toxic elements present in road dust from industrial areas in korea." *Atmosphere* 11 (12):16. doi: 10.3390/atmos11121366.

Jiang, Y. B., S. Matsusaka, H. Masuda, and Y. Qian. 2008. "Characterizing the effect of substrate surface roughness on particle-wall interaction with the airflow method." *Powder Technology* 186 (3):199-205. doi: 10.1016/j.powtec.2007.11.041.

Kim, Y., G. Wellum, K. Mello, K. E. Strawhecker, R. Thoms, A. Giaya, and B. E. Wyslouzil. 2016. "Effects of relative humidity and particle and surface properties on particle resuspension rates." *Aerosol Science and Technology* 50 (4):339-352. doi: 10.1080/02786826.2016.1152350.

Knibbs, L. D., C. R. He, C. Duchaine, and L. Morawska. 2012. "Vacuum cleaner emissions as a source of indoor exposure to airborne particles and bacteria." *Environmental Science & Technology* 46 (1):534-542. doi: 10.1021/es202946w.

Kvasnicka, J., E. A. C. Hubal, J. A. Siegel, J. A. Scott, and M. L. Diamond. 2022. "Modeling clothing as a vector for transporting airborne particles and pathogens across indoor microenvironments." *Environmental Science & Technology* 56 (9):5641-5652. doi: 10.1021/acs.est.1c08342.

Lai, A. C. K., Y. L. Tian, J. Y. L. Tsoi, and A. R. Ferro. 2017. "Experimental study of the effect of shoes on particle resuspension from indoor flooring materials." *Building and Environment* 118:251-258. doi: 10.1016/j.buildenv.2017.02.024.

Lee, H. H., Y. S. Cheung, S. C. Fu, and C. Y. H. Chao. 2019. "Study of particle resuspension from dusty surfaces using a centrifugal method." *Indoor Air* 29 (5):791-802. doi: 10.1111/ina.12576.

Leung, C. C. D., C. M. Ngai, C. K. Wong, and Y. H. Chan. 2023. "A rare case of melioidosis presenting as pericarditis and pneumonia in a patient with poorly controlled diabetes mellitus." *Respirology Case Reports* 11 (4):3. doi: 10.1002/rcr2.1119.

Leung, W. T., S. C. Fu, and C. Y. H. Chao. 2017. "Detachment of droplets by air jet impingement." *Aerosol Science and Technology* 51 (4):467-476. doi: 10.1080/02786826.2016.1265911.

Licina, D., and W. W. Nazaroff. 2018. "Clothing as a transport vector for airborne particles: Chamber study." *Indoor Air* 28 (3):404-414. doi: 10.1111/ina.12452.

Nasr, B., G. Ahmadi, A. R. Ferro, and S. Dhaniyala. 2020. "A model for particle removal from surfaces with large-scale roughness in turbulent flows." *Aerosol Science and Technology* 54 (3):291-303. doi: 10.1080/02786826.2019.1692126.

Pace, R., G. Guidolotti, C. Baldacchini, E. Pallozzi, R. Grote, D. J. Nowak, and C. Calfapietra. 2021. "Comparing i-tree eco estimates of particulate matter deposition with leaf and canopy measurements in an urban mediterranean holm oak forest." *Environmental Science & Technology* 55 (10):6613-6622. doi: 10.1021/acs.est.0c07679.

Qi, Y., Y. C. Chen, X. Yan, W. Liu, L. Ma, Y. C. Liu, Q. X. Ma, and S. J. Liu. 2022. "Co-exposure of ambient particulate matter and airborne transmission pathogens: The impairment of the upper respiratory systems." *Environmental Science & Technology*:10. doi: 10.1021/acs.est.2c03856.

Reeks, M. W., and D. Hall. 2001. "Kinetic models for particle resuspension in turbulent flows: Theory and measurement." *Journal of Aerosol Science* 32 (1):1-31. doi: 10.1016/s0021-8502(00)00063-x.

Reeks, M. W., J. Reed, and D. Hall. 1988. "On the resuspension of small particles by a turbulent-flow." *Journal of Physics D-Applied Physics* 21 (4):574-589. doi: 10.1088/0022-3727/21/4/006.

Rienda, I. C., and C. A. Alves. 2021. "Road dust resuspension: A review." *Atmospheric Research* 261:24. doi: 10.1016/j.atmosres.2021.105740.

Roberts, J. W., G. Glass, and L. Mickelson. 2004. "A pilot study of the measurement and control of deep dust, surface dust, and lead in 10 old carpets using the 3-spot test while vacuuming." *Archives of Environmental Contamination and Toxicology* 48 (1):16-23. doi: 10.1007/s00244-003-0224-0.

Rondeau, A., S. Peillon, A. M. Vidales, J. Benito, R. Unac, J. C. Sabroux, and F. Gensdarmes. 2021. "Evidence of inter-particles collision effect in airflow resuspension of poly-dispersed non-spherical tungsten particles in monolayer deposits." *Journal of Aerosol Science* 154:16. doi: 10.1016/j.jaerosci.2020.105735.

Shiraiwa, M., K. Ueda, A. Pozzer, G. Lammel, C. J. Kampf, A. Fushimi, S. Enami, A. M. Arangio, J. Frohlich-Nowoisky, Y. Fujitani, A. Furuyama, P. S. J. Lakey, J. Lelieveld, K. Lucas, Y. Morino, U. Poschl, S. Takaharna, A. Takami, H. J. Tong, B. Weber, A. Yoshino, and K. Sato. 2017. "Aerosol health effects from molecular to global scales." *Environmental Science & Technology* 51 (23):13545-13567. doi: 10.1021/acs.est.7b04417.

Song, J., R. R. Qu, B. B. Sun, R. J. Chen, H. D. Kan, Z. An, J. Jiang, J. Li, Y. G. Zhang, and W. D. Wu. 2022. "Associations of short-term exposure to fine particulate matter with neural damage biomarkers: A panel study of healthy retired adults." *Environmental Science & Technology* 56 (11):7203-7213. doi: 10.1021/acs.est.1c03754.

Sun, S. Z., W. N. Cao, V. C. Pun, H. Qiu, Y. Ge, and L. W. Tian. 2019. "Respirable particulate constituents and risk of cause-specific mortality in the hong kong population." *Environmental Science & Technology* 53 (16):9810-9817. doi: 10.1021/acs.est.9b01635.

Theron, F., D. Debba, and L. Le Coq. 2020. "Local experimental methodology for the study of microparticles resuspension in ventilated duct during fan acceleration." *Journal of Aerosol Science* 140:17. doi: 10.1016/j.jaerosci.2019.105477.

Theron, F., D. Debba, and L. Le Coq. 2022. "Influence of the transient airflow pattern on the temporal evolution of microparticle resuspension: Application to ventilated duct during fan acceleration." *Aerosol Science and Technology* 56 (11):1033-1046. doi: 10.1080/02786826.2022.2120793.

Wu, T. R., M. J. Fu, M. Valkonen, M. Taubel, Y. Xu, and B. E. Boor. 2021. "Particle resuspension dynamics in the infant near-floor microenvironment." *Environmental Science & Technology* 55 (3):1864-1875. doi: 10.1021/acs.est.0c06157.

Wu, Y. L., C. I. Davidson, and A. G. Russell. 1992. "Controlled wind-tunnel experiments for particle bounceoff and resuspension." *Aerosol Science and Technology* 17 (4):245-262. doi: 10.1080/02786829208959574.

You, S. M., and M. P. Wan. 2014. "A new turbulent-burst-based model for particle resuspension from rough surfaces in turbulent flow." *Aerosol Science and Technology* 48 (10):1031-1042. doi: 10.1080/02786826.2014.955908.

Zhang, X. L., X. Chen, Y. Yue, S. X. Wang, B. Zhao, X. M. Huang, T. T. Li, Q. H. Sun, and J. Wang. 2023. "Ecological study on global health effects due to source-specific ambient fine particulate matter exposure." *Environmental Science & Technology*:14. doi: 10.1021/acs.est.2c06752.

Zhang, X. Y., J. Y. Lyu, Y. J. Han, N. X. Sun, W. Sun, J. M. Li, C. J. Liu, and S. Yin. 2020. "Effects of the leaf functional traits of coniferous and broadleaved trees in subtropical monsoon regions on pm2.5 dry deposition velocities." *Environmental Pollution* 265:10. doi: 10.1016/j.envpol.2020.114845.

Zhou, N. Y., C. T. Jiang, Q. Chen, H. Yang, X. G. Wang, P. Zou, L. Sun, J. J. Liu, L. Li, L. B. Li, L. P. Huang, H. Q. Chen, L. Ao, Z. Y. Zhou, J. Y. Liu, Z. H. Cui, and J. Cao. 2018. "Exposures to atmospheric pm10 and pm10-2.5 affect male semen quality: Results of marhcs study." *Environmental Science & Technology* 52 (3):1571-1581. doi: 10.1021/acs.est.7b05206.

Ziskind, G., M. Fichman, and C. Gutfinger. 1997. "Adhesion moment model for estimating particle detachment from a surface." *Journal of Aerosol Science* 28 (4):623-634. doi: 10.1016/s0021-8502(96)00460-0.

Captions

Figure 1. Schematic diagram of the experimental setup. (a) Front view of the working section of the wind tunnel. (b) SEM images of the fabrics. (c) The setup of dust deposition. (d) Air velocity versus time. Cotton was chosen as a representative to be shown here because all fabrics share similar trends in this study. All resuspension experiments were performed in triplicate, and data are expressed as the mean ± standard deviation. Solid lines + solid symbols represent the moving fabric case, and dashed lines + open symbols represent the fixed fabric case.

Figure 2. Remaining fraction versus $\ln(U/U_C)^3$ with respect to different fabric types. (a) Cotton. (b) Linen. (c) Silk. (d) Polyester. All resuspension experiments were performed in triplicate, and data are expressed as the mean ± standard deviation. The solid curves represent Eq. (2a) for $n = 1, 2, 3$, and the dashed curves represent the estimation using Eq. (2a) for the special case of $n = 0$.

Figure 3. Remaining fraction (at $t = t_0$) versus $\ln(U/U_C)^3$ with respect to different fabric types. (a) Cotton. (b) Linen. (c) Silk. (d) Polyester. All resuspension experiments were performed in triplicate, and data are expressed as the mean ± standard deviation. The dashed curves represent the estimation using Eq. (2a) for the special case of $n = 0$, and the solid curves represent the modified equation, Eq. (2b), for $n = 0$.

Figure 4. Difference in remaining fractions, ΔRF ($= RF_{fixed\ case} - RF_{moving\ case}$) versus air velocity with respect to different fabric types. (a) Cotton. (b) Linen. (c) Silk. (d) Polyester. All resuspension experiments were performed in triplicate, and data are expressed as the mean ± standard deviation.

Figure 5. Flow-induced fabric motion analysis. (a) Stacked images of traces (the moving cotton fabric at $U = 4$ m/s and $U = 6$ m/s) within different time periods. (b) Fabric acceleration (P6 on the cotton fabric at $U = 4$ m/s and $U = 6$ m/s) versus time. The numbers with the same color as the curves represent the maximum accelerations of the curves within each 5 s. (c) Partial enlargement of Figure b. (d) Cube of critical velocity versus longitudinal flexural rigidity.

Figure 6. Remaining fraction versus fabric maximum acceleration. All resuspension experiments were performed in triplicate, and data are expressed as the mean ± standard deviation. An exponentially decaying trendline is drawn as a guide to the eye.

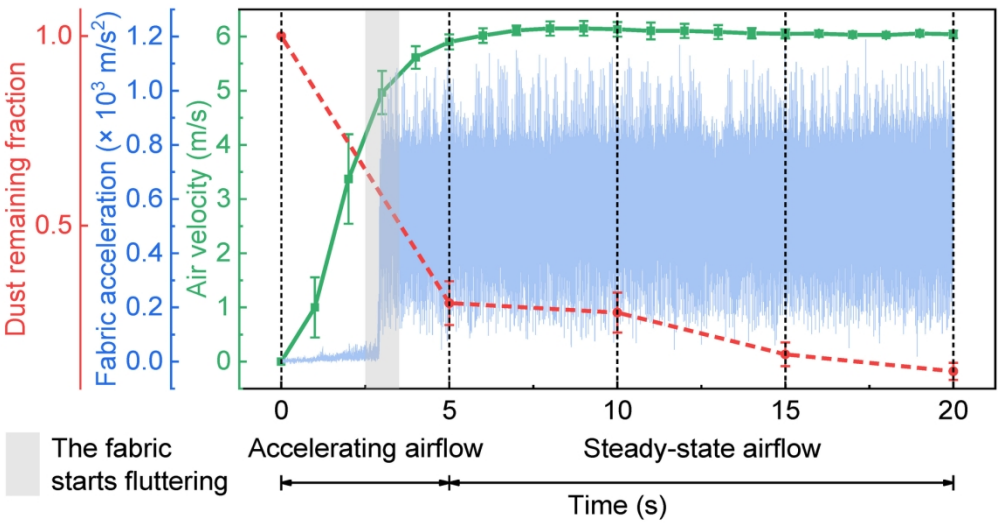

83x44mm (600 x 600 DPI)

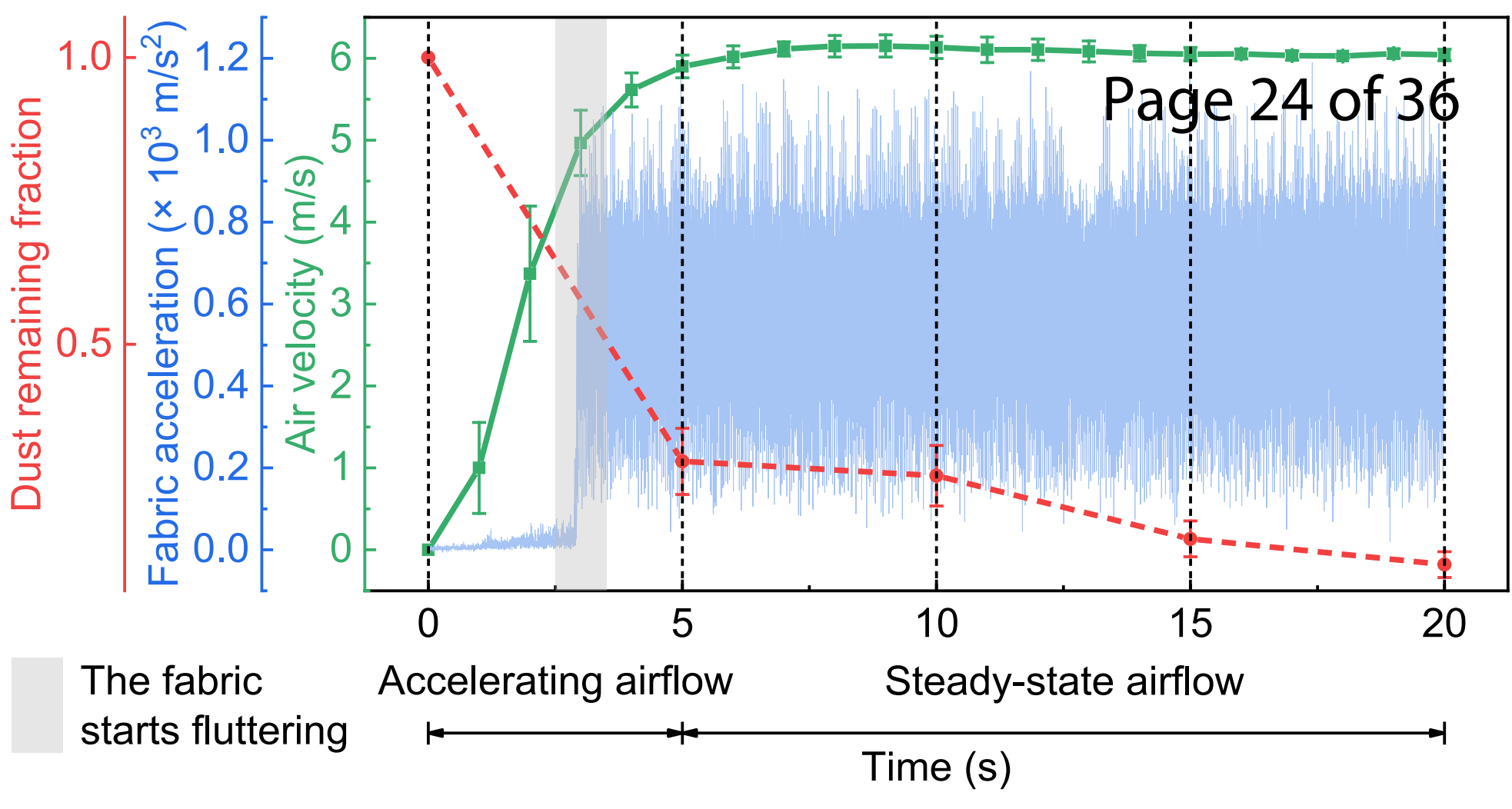
Dust remaining fraction
1.0
0.5
Fabric acceleration (× 10³ m/s²)
1.2
1.0
0.8
0.6
0.4
0.2
0.0
Air velocity (m/s)
6
5
4
3
2
1
0
Page 24 of 36
0
5
10
15
20
The fabric starts fluttering
Accelerating airflow
Steady-state airflow
Time (s)

a

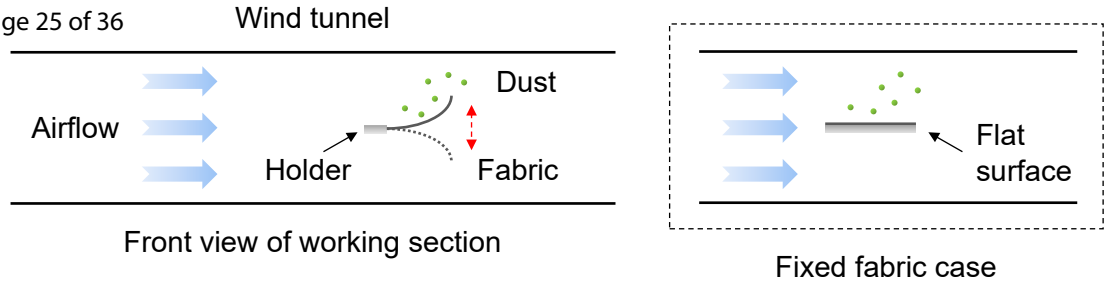
Wind tunnel
Airflow
Dust
Holder
Fabric
Front view of working section
Flat surface
Fixed fabric case

b

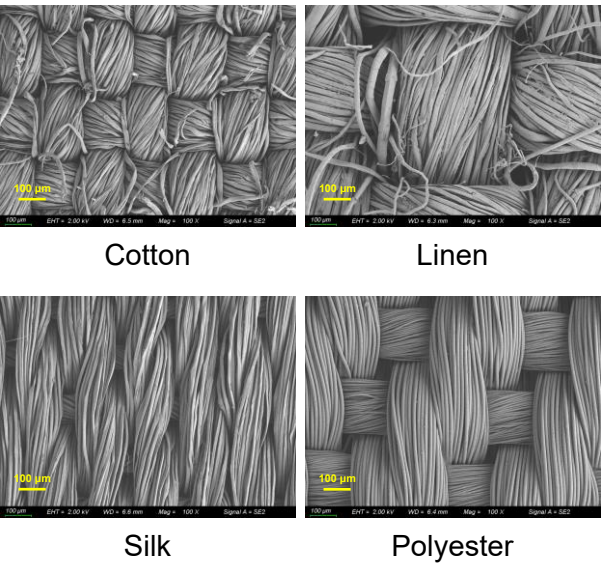
Cotton
Linen
Silk
Polyester

d

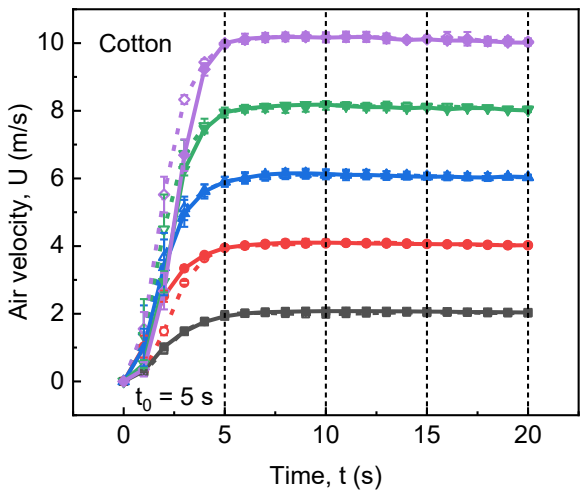
Cotton
Air velocity, U (m/s)
Time, t (s)
t_0 = 5 s
0
2
4
6
8
10
0
5
10
15
20

c

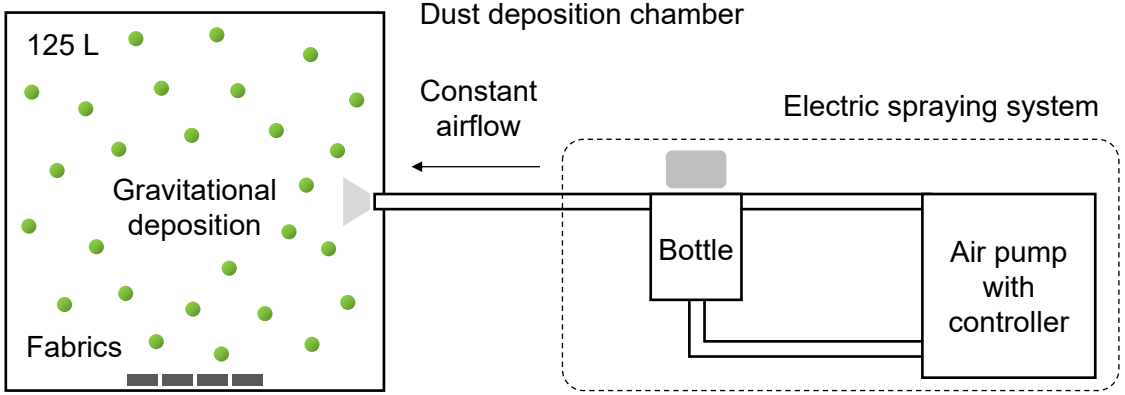
125 L
Gravitational deposition
Fabrics
Dust deposition chamber
Constant airflow
Electric spraying system
Bottle
Air pump with controller

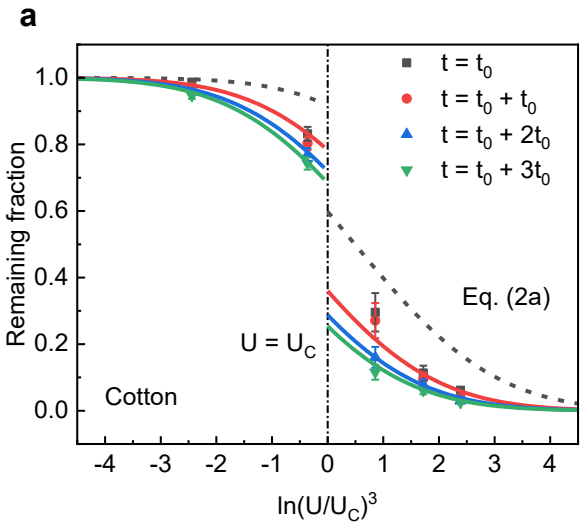
a
Remaining fraction
1.0
0.8
0.6
0.4
0.2
0.0
-4 -3 -2 -1 0 1 2 3 4
ln(U/U_C)^3
t = t_0
t = t_0 + t_0
t = t_0 + 2t_0
t = t_0 + 3t_0
Eq. (2a)
U = U_C
Cotton

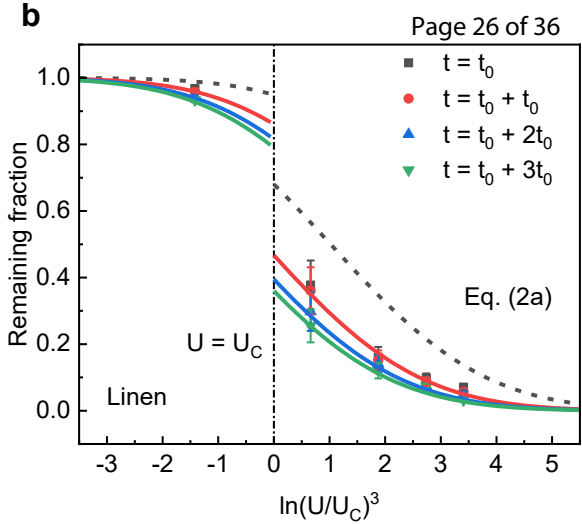
b
Remaining fraction
1.0
0.8
0.6
0.4
0.2
0.0
-3 -2 -1 0 1 2 3 4 5
ln(U/U_C)^3
t = t_0
t = t_0 + t_0
t = t_0 + 2t_0
t = t_0 + 3t_0
Eq. (2a)
U = U_C
Linen

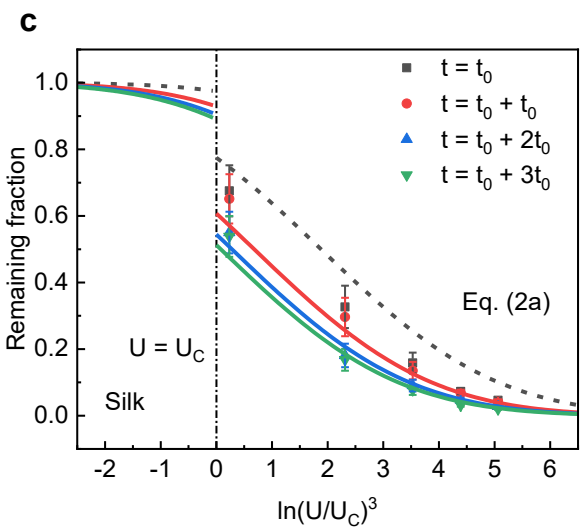
c
Remaining fraction
1.0
0.8
0.6
0.4
0.2
0.0
-2 -1 0 1 2 3 4 5 6
ln(U/U_C)^3
t = t_0
t = t_0 + t_0
t = t_0 + 2t_0
t = t_0 + 3t_0
Eq. (2a)
U = U_C
Silk

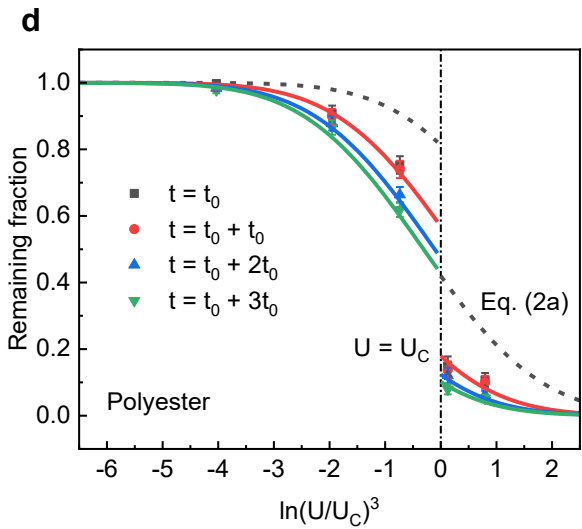
d
Remaining fraction
1.0
0.8
0.6
0.4
0.2
0.0
-6 -5 -4 -3 -2 -1 0 1 2
ln(U/U_C)^3
t = t_0
t = t_0 + t_0
t = t_0 + 2t_0
t = t_0 + 3t_0
Eq. (2a)
U = U_C
Polyester

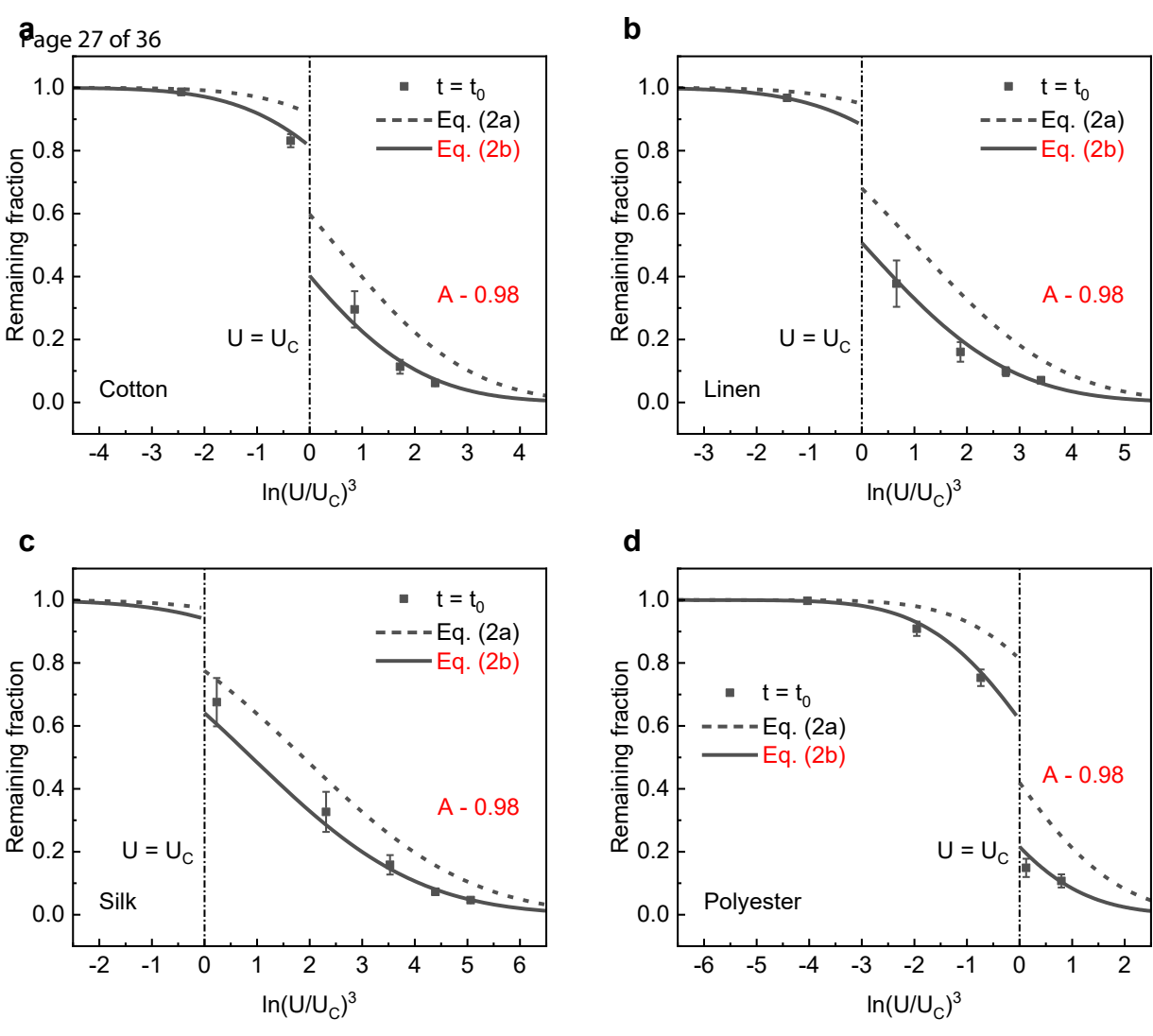
a
Remaining fraction
1.0
0.8
0.6
0.4
0.2
0.0
t = t0
Eq. (2a)
Eq. (2b)
A - 0.98
U = UC
Cotton
-4 -3 -2 -1 0 1 2 3 4
ln(U/UC)3
b
Remaining fraction
t = t0
Eq. (2a)
Eq. (2b)
A - 0.98
U = UC
Linen
-3 -2 -1 0 1 2 3 4 5
ln(U/UC)3
c
Remaining fraction
t = t0
Eq. (2a)
Eq. (2b)
A - 0.98
U = UC
Silk
-2 -1 0 1 2 3 4 5 6
ln(U/UC)3
d
Remaining fraction
t = t0
Eq. (2a)
Eq. (2b)
A - 0.98
U = UC
Polyester
-6 -5 -4 -3 -2 -1 0 1 2
ln(U/UC)3

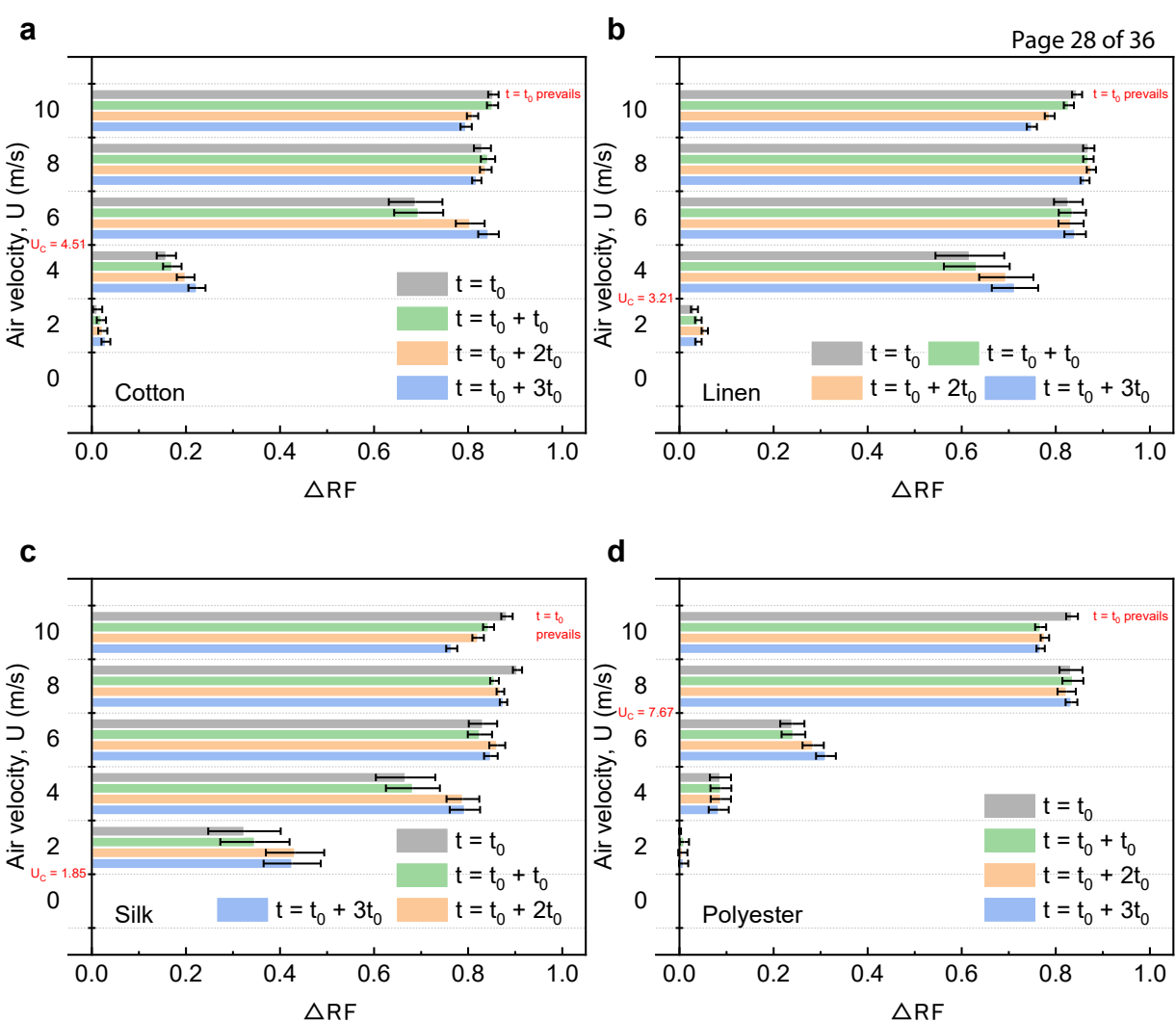
a
Air velocity, U (m/s)
t = t0 prevails
Uc = 4.51
t = t0
t = t0 + t0
t = t0 + 2t0
t = t0 + 3t0
Cotton
△RF
b
Air velocity, U (m/s)
t = t0 prevails
Uc = 3.21
t = t0
t = t0 + t0
t = t0 + 2t0
t = t0 + 3t0
Linen
△RF
c
Air velocity, U (m/s)
t = t0 prevails
Uc = 1.85
t = t0
t = t0 + t0
t = t0 + 2t0
t = t0 + 3t0
Silk
△RF
d
Air velocity, U (m/s)
t = t0 prevails
Uc = 7.67
t = t0
t = t0 + t0
t = t0 + 2t0
t = t0 + 3t0
Polyester
△RF

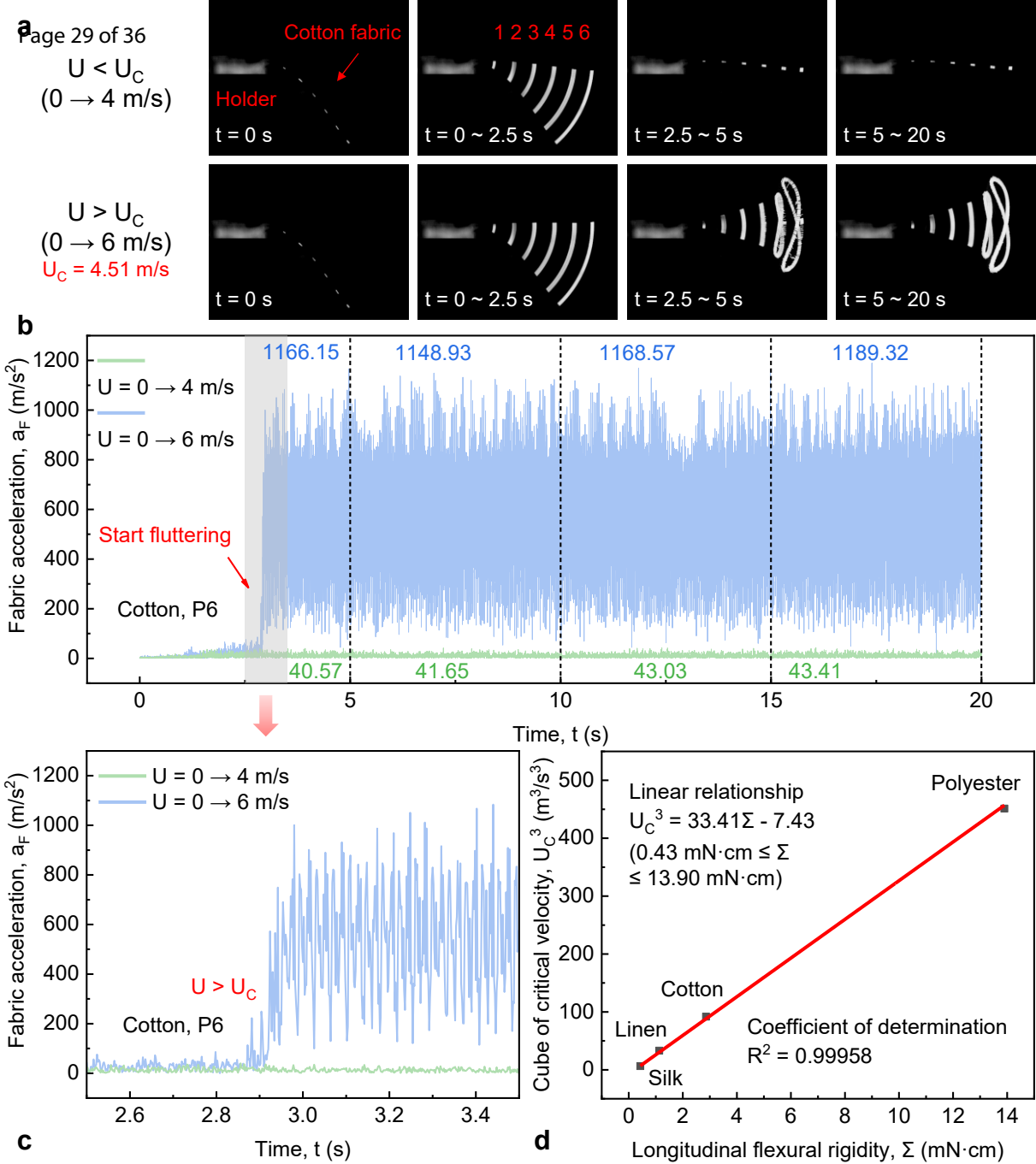
a
U < U_C
(0 → 4 m/s)
Cotton fabric
Holder
1 2 3 4 5 6
t = 0 s
t = 0 ~ 2.5 s
t = 2.5 ~ 5 s
t = 5 ~ 20 s
U > U_C
(0 → 6 m/s)
U_C = 4.51 m/s
t = 0 s
t = 0 ~ 2.5 s
t = 2.5 ~ 5 s
t = 5 ~ 20 s
b
Fabric acceleration, a_F (m/s²)
U = 0 → 4 m/s
U = 0 → 6 m/s
Start fluttering
Cotton, P6
1166.15
1148.93
1168.57
1189.32
40.57
41.65
43.03
43.41
Time, t (s)
c
Fabric acceleration, a_F (m/s²)
U = 0 → 4 m/s
U = 0 → 6 m/s
U > U_C
Cotton, P6
Time, t (s)
d
Cube of critical velocity, U_C³ (m³/s³)
Linear relationship
U_C³ = 33.41Σ - 7.43
(0.43 mN·cm ≤ Σ
≤ 13.90 mN·cm)
Polyester
Cotton
Linen
Silk
Coefficient of determination
R² = 0.99958
Longitudinal flexural rigidity, Σ (mN·cm)

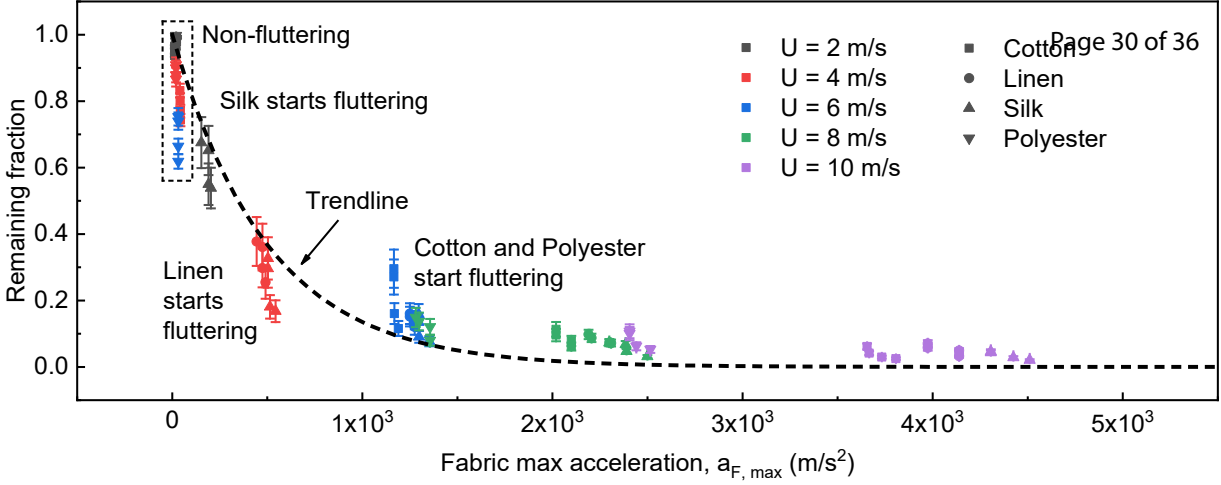
Non-fluttering
Silk starts fluttering
Trendline
Linen
starts
fluttering
Cotton and Polyester
start fluttering
U = 2 m/s
U = 4 m/s
U = 6 m/s
U = 8 m/s
U = 10 m/s
Cotton
Linen
Silk
Polyester
Remaining fraction
1.0
0.8
0.6
0.4
0.2
0.0
0
1x10^3
2x10^3
3x10^3
4x10^3
5x10^3
Fabric max acceleration, a_F, max (m/s^2)

Supplemental Information

Dust Resuspension from Fabrics Exposed to Airflow

Jie Feng [a], Tsz Wai Lai [b], Sau Chung Fu [b, *], Ka Chung Chan [b], Chun-Ho Liu [a], Christopher Y.H. Chao [b, c]

[a] Department of Mechanical Engineering, The University of Hong Kong, Hong Kong, China

[b] Department of Building Environment and Energy Engineering, The Hong Kong Polytechnic University, Hong Kong, China

[c] Department of Mechanical Engineering, The Hong Kong Polytechnic University, Hong Kong, China

[*] Corresponding author. E-mail address: schung.fu@polyu.edu.hk (S.C. Fu).

Table S1. Initial dust loads on fabrics in all resuspension experiments. Some field investigations have reported dust loads ranging from 0.7 ~ 21.1 g/m^2 (Wu et al. 2021; Roberts et al. 2004) and 15 ~ 1669 g/m^2 (Jeong et al. 2020; Gustafsson et al. 2019) in indoor and outdoor environments respectively. Therefore, a dust load level of 15 g/m^2 was moderately selected for our study. A consistent dust deposition method was used to ensure an initial dust load of approximately 15 g/m^2 on each fabric in all resuspension experiments. The results below demonstrate its uniformity and repeatability in this study. The fabric weight before and after dust deposition was measured using an analytical balance (ABP 200-5DM, Kern, Germany), allowing the initial dust load to be obtained. The associated uncertainties may be due to measurement errors and fabric surface differences.

Fabric type	Initial dust load (mean ± standard deviation) [g/m^2]
Cotton	15.02 ± 0.34
Linen	15.88 ± 0.49
Silk	15.01 ± 0.42
Polyester	15.46 ± 0.39

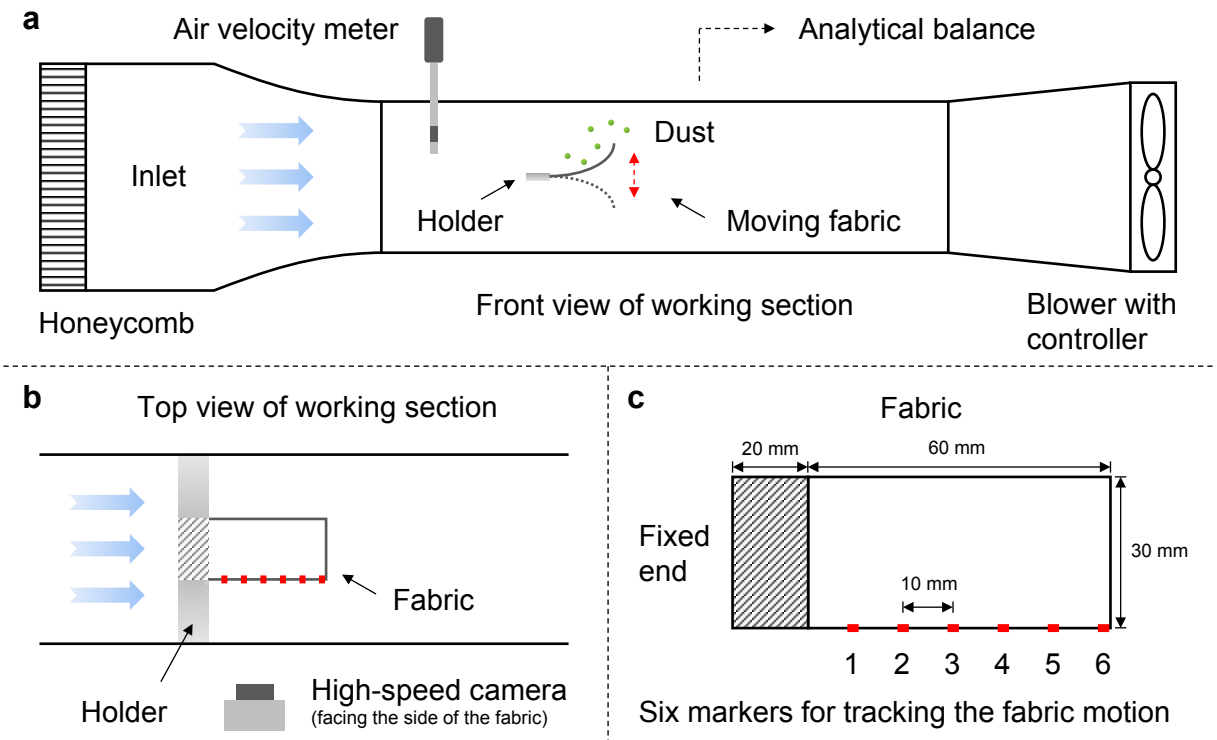

Figure S1. Detailed experimental setup. (a) The wind tunnel for dust resuspension experiments. (b) Top view of the working section. (c) Fabric dimensions.

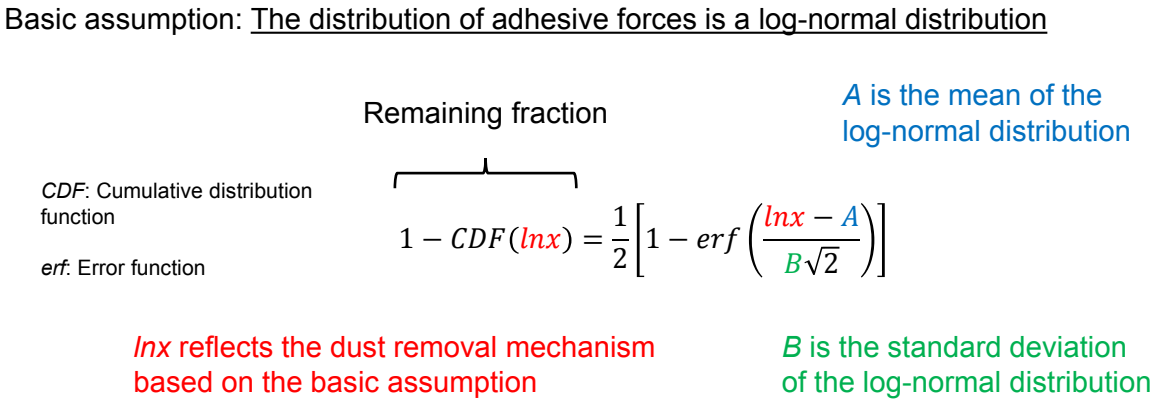

Figure S2. Basic form of Equation 2. The basic assumption and mathematical description were derived from our previous work (Leung et al. 2017; Fu et al. 2013). The remaining fraction (our dependent variable) was expressed as 1 – CDF, while the natural logarithm of a dimensionless term (our independent variable related to air velocity) was chosen to reflect the dust removal mechanism based on the basic assumption in this study. A and B can be affected by our experimental factors, such as fabric type and airflow duration. By fitting our experimental results, their optimal expressions were derived, as shown in Eq. (2) in the original article.

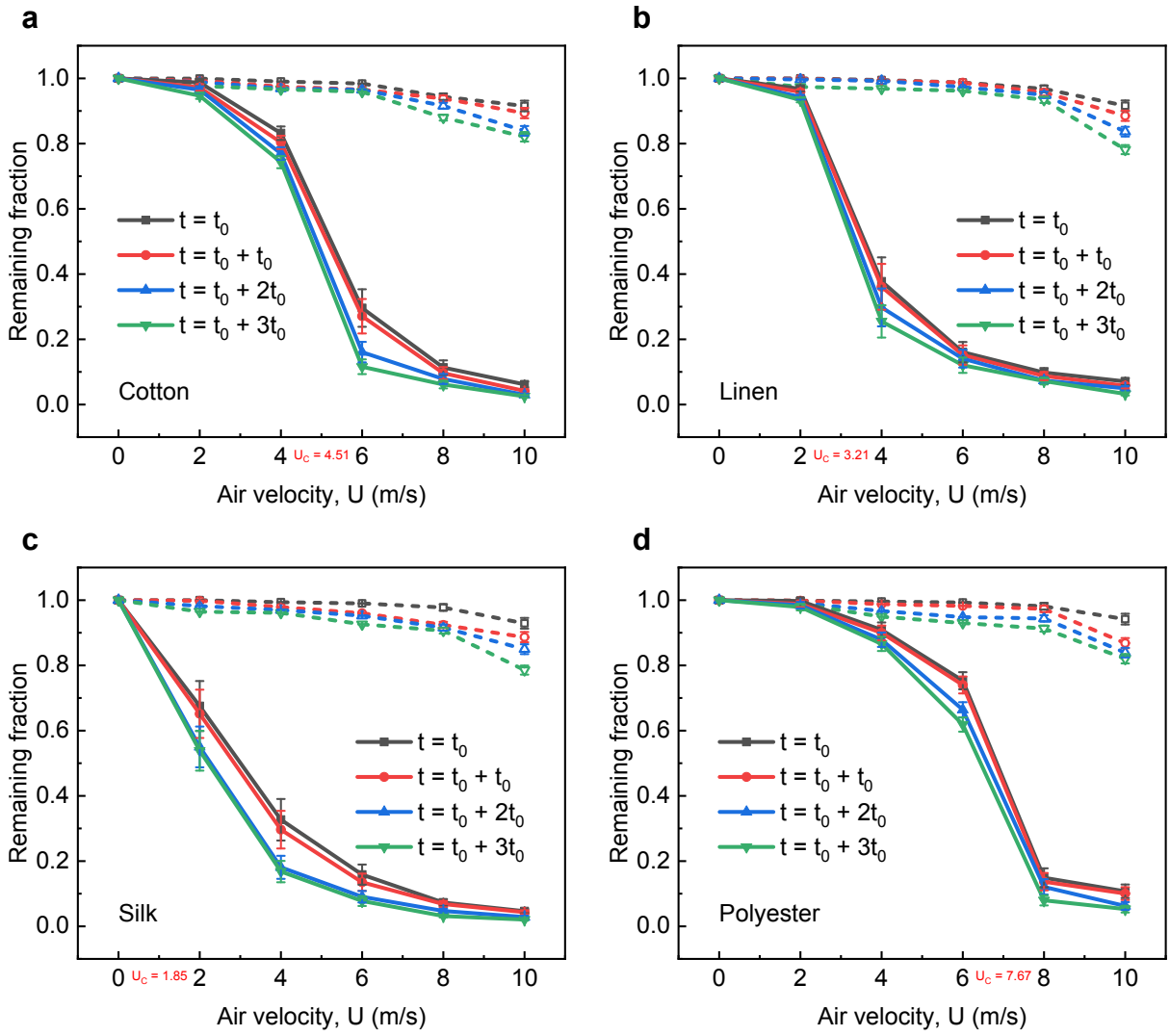

Figure S3. Remaining fraction versus air velocity with respect to different fabric types. All resuspension experiments were performed in triplicate, and data are expressed as the mean ± standard deviation. Solid lines + solid symbols represent the moving fabric case, and dashed lines + open symbols represent the fixed fabric case.

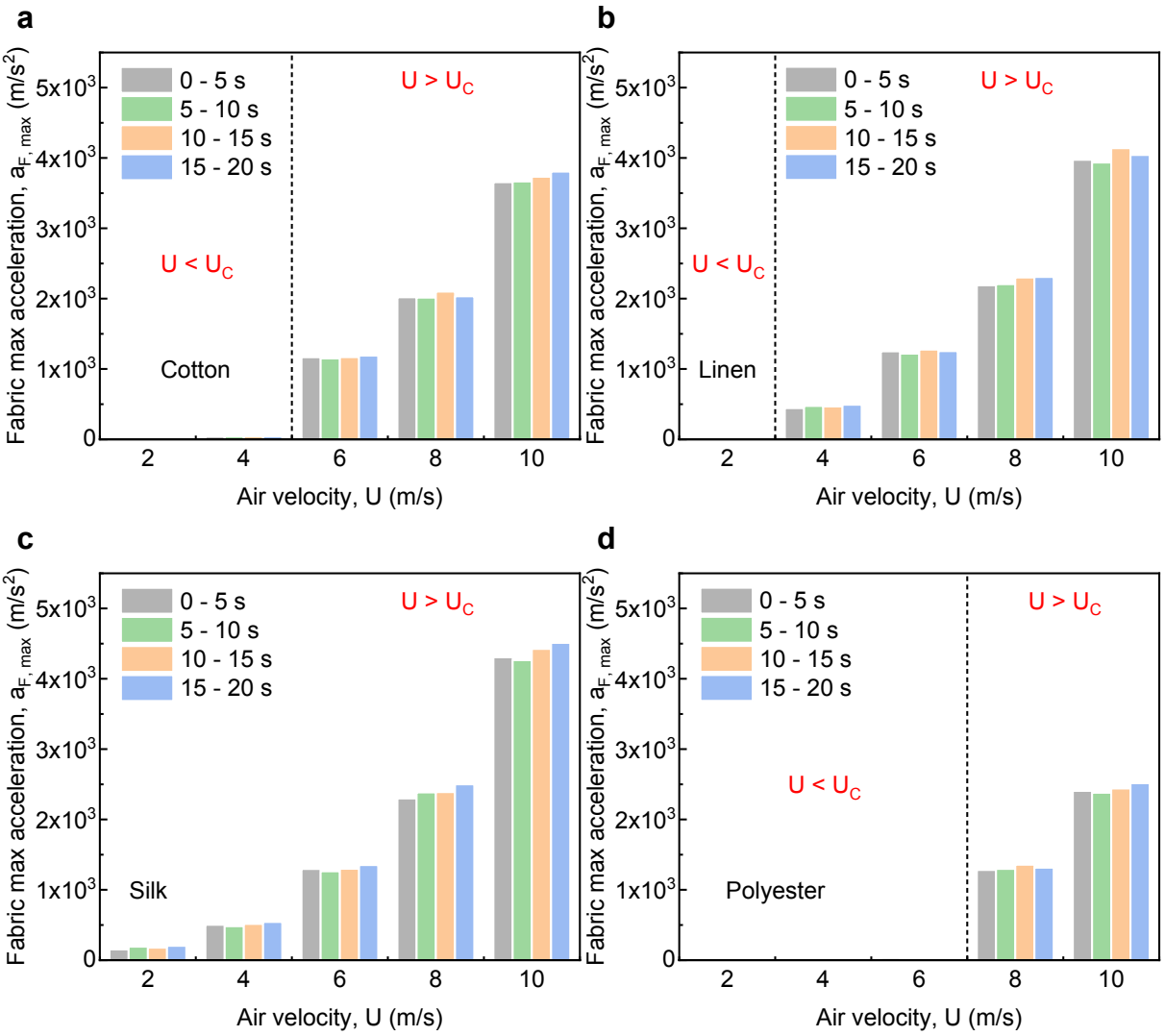

Figure S4. Fabric maximum acceleration (P6) within 5-second interval versus air velocity with respect to different fabric types. (a) Cotton. (b) Linen. (c) Silk. (d) Polyester.

References

Fu, S. C., C. Y. H. Chao, R. M. C. So, and W. T. Leung. 2013. "Particle resuspension in a wall-bounded turbulent flow." *Journal of Fluids Engineering-Transactions of the Asme* 135 (4):9. doi: 10.1115/1.4023660.

Gustafsson, M., G. Blomqvist, I. Jarlskog, J. Lundberg, S. Janhall, M. Elmgren, C. Johansson, M. Norman, and S. Silvergren. 2019. "Road dust load dynamics and influencing factors for six winter seasons in stockholm, sweden." *Atmospheric Environment-X* 2:12. doi: 10.1016/j.aeaoa.2019.100014.

Jeong, H., J. Y. Choi, J. Lim, and K. Ra. 2020. "Pollution caused by potentially toxic elements present in road dust from industrial areas in korea." *Atmosphere* 11 (12):16. doi: 10.3390/atmos11121366.

Leung, W. T., S. C. Fu, and C. Y. H. Chao. 2017. "Detachment of droplets by air jet impingement." *Aerosol Science and Technology* 51 (4):467-476. doi: 10.1080/02786826.2016.1265911.

Roberts, J. W., G. Glass, and L. Mickelson. 2004. "A pilot study of the measurement and control of deep dust, surface dust, and lead in 10 old carpets using the 3-spot test while vacuuming." *Archives of Environmental Contamination and Toxicology* 48 (1):16-23. doi: 10.1007/s00244-003-0224-0.

Wu, T. R., M. J. Fu, M. Valkonen, M. Taubel, Y. Xu, and B. E. Boor. 2021. "Particle resuspension dynamics in the infant near-floor microenvironment." *Environmental Science & Technology* 55 (3):1864-1875. doi: 10.1021/acs.est.0c06157.